A data-driven approach to π^0, η and η' Dalitz decays

Rafel Escribano
Universitat Autònoma de Barcelona

MESON 2016
14th International Workshop on
Meson Production, Properties and Interaction

June 3, 2016
Auditorium Maximum, Kraków (Poland)

Purpose:

To present an analysis of the π^0, η and η' single and double Dalitz decays by means of a data-driven model-independent approach based on the use of rational approximants

Motivations:

- To explore further applications of the η and η' transition form factors obtained from experimental data at low and intermediate energies in the space-like region
- To calculate the dilepton invariant mass spectra and branching ratios of these Dalitz decays in order to provide predictions for present and future experimental colls.

Outline:

- *Pseudoscalar transition form factors*
- *Padé approximants*
- *Application to η and η' TFFs*
- *Results*
- *Single Dalitz decays*
- *Double Dalitz decays*
- *Conclusions*

In collab. with P. Masjuan, P. Sánchez-Puertas (Mainz) and S. Gonzàlez-Solís (UAB)
Phys. Rev. D89 (2014) 3, 034014 and arXiv:1512.07520 [hep-ph]

• *Pseudoscalar transition form factors (space-like region)*

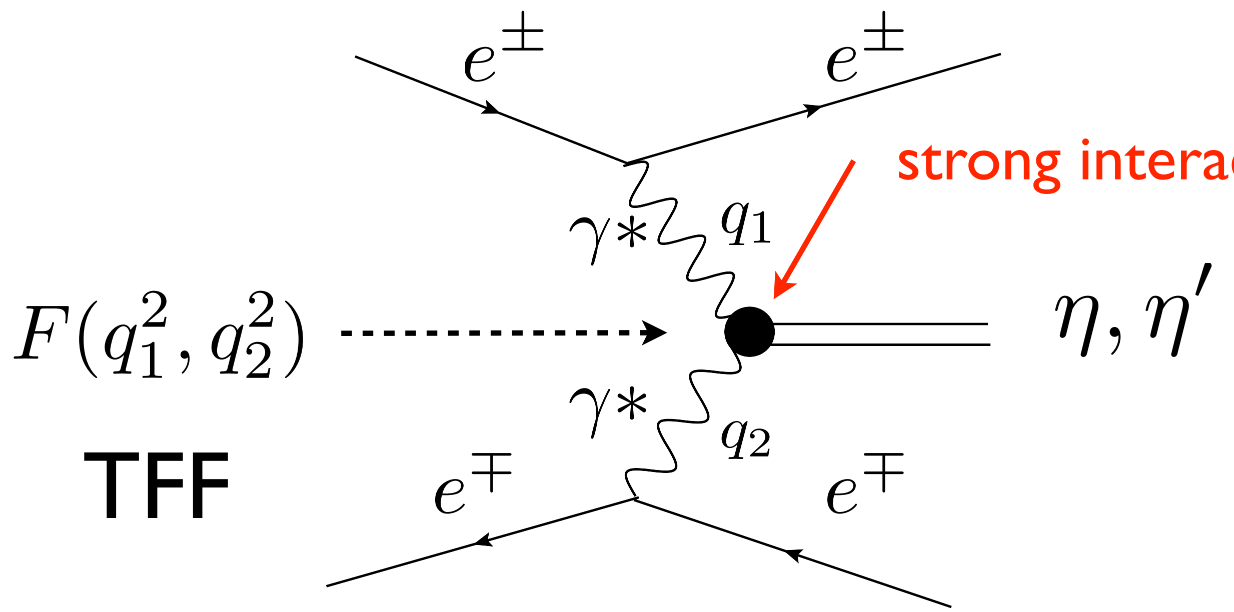

not exp. accesible

Single Tag Method

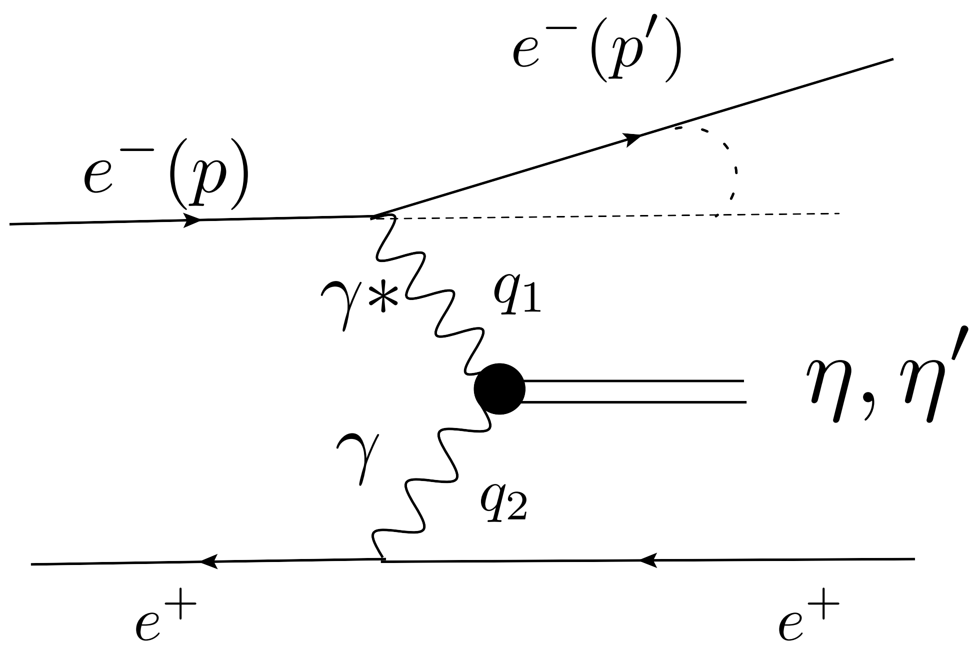

$$F_{P\gamma^*\gamma}(Q^2) \equiv F_{P\gamma^*\gamma^*}(-Q^2, 0)$$

Momentum transfer

- highly virtual photon ⇒ tagged
- quasi-real photon ⇒ untagged

Selection criteria

- 1 e^- detected
- 1 e^+ along beam axis
- Meson full reconstructed

• *Pseudoscalar transition form factors*

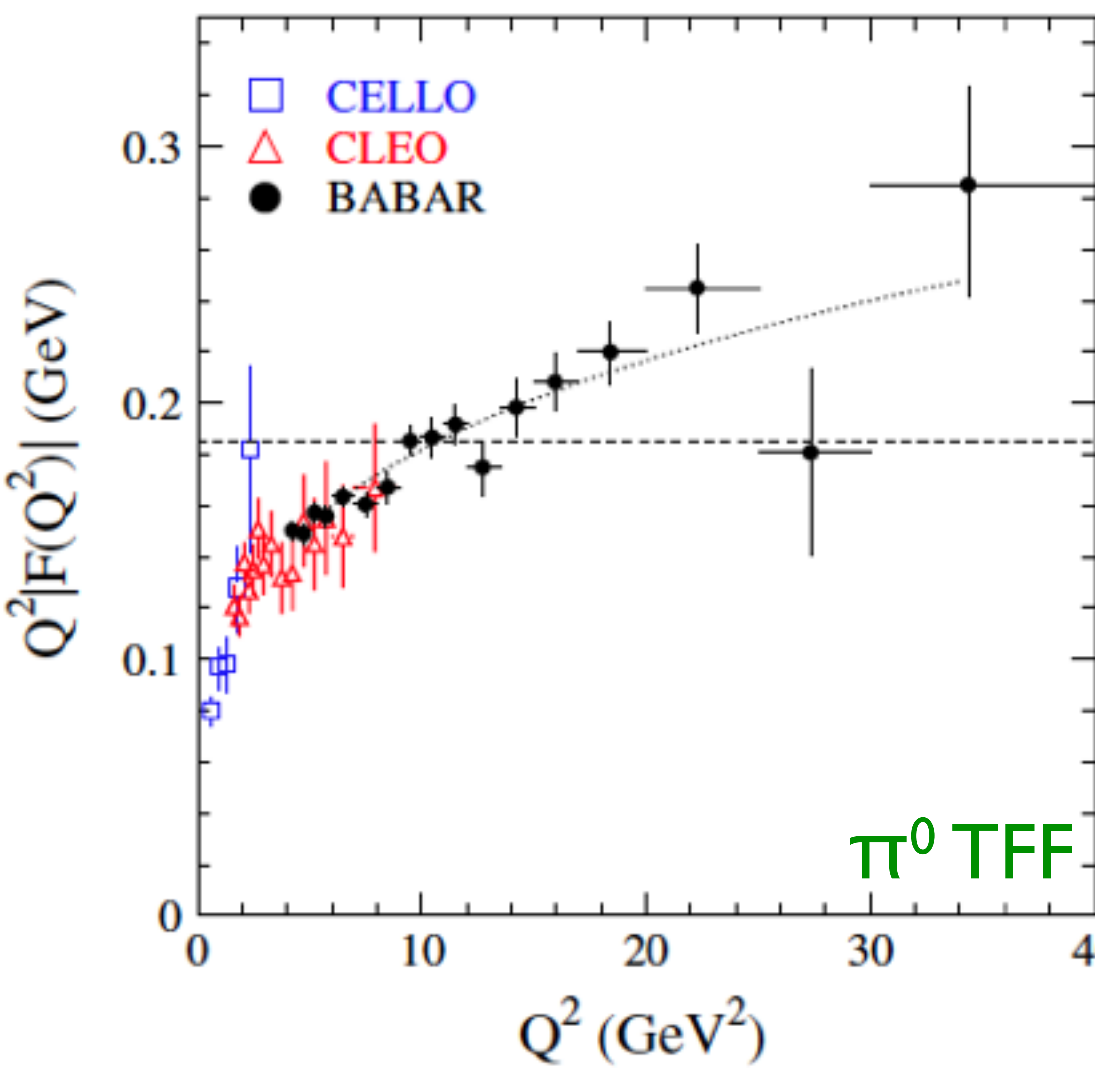

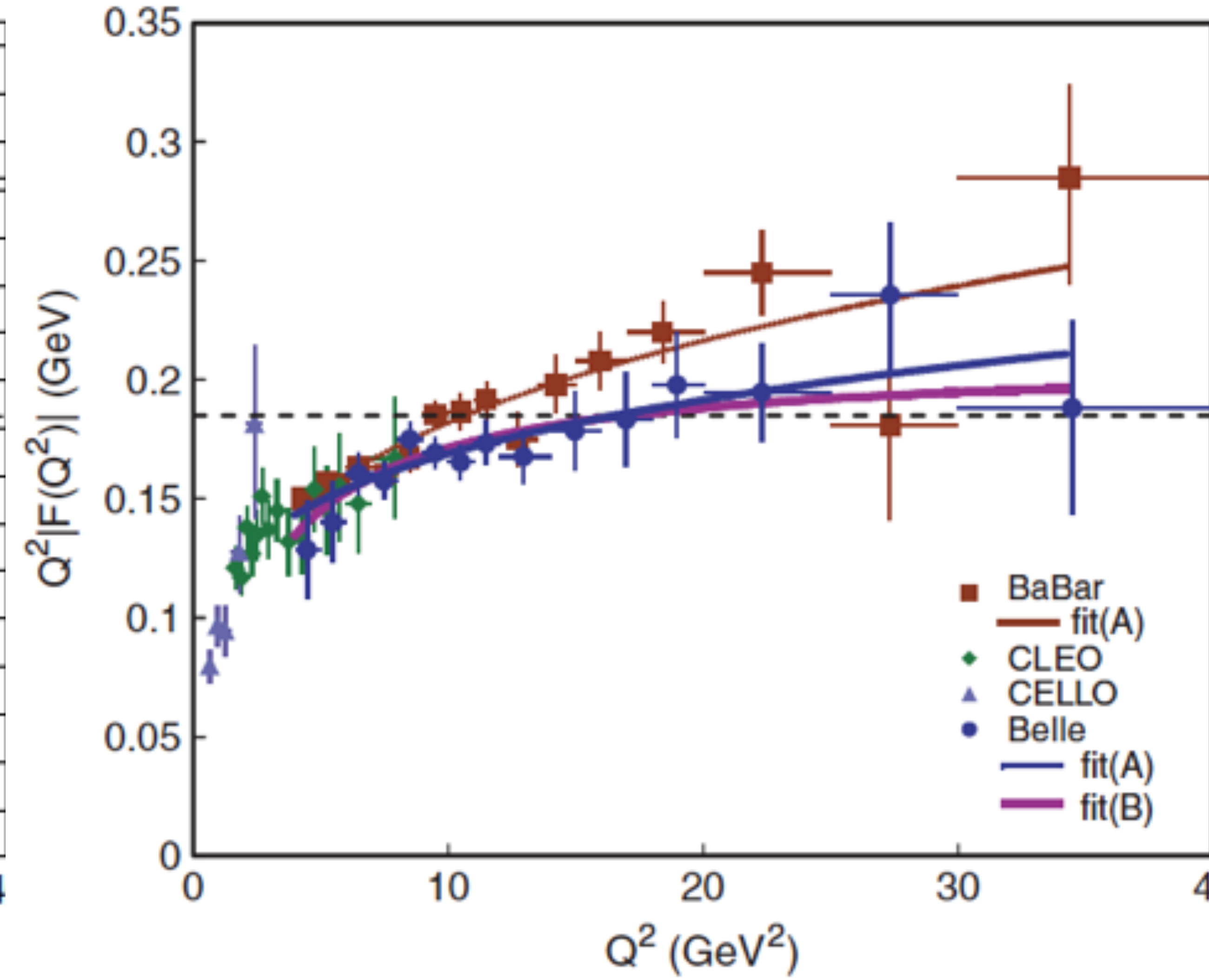

S. Uehara et al. (BELLE Collaboration), PRD 86 (2012) 092007

FIG. 22 (color online). The $\gamma\gamma^* \to \pi^0$ transition form factor multiplied by Q^2. The dashed line indicates the asymptotic limit for the form factor. The dotted curve shows the interpolation given by Eq. (9).

B. Aubert et al. (BABAR Collaboration), PRD 80 (2009) 052002

- *Pseudoscalar transition form factors*

@ low-momentum transfer:

slope

$$F_{P\gamma^*\gamma}(Q^2) = F_{P\gamma\gamma}(0)\left(1 - b_P\frac{Q^2}{m_P^2} + c_P\frac{Q^4}{m_P^4} + \cdots\right)$$

curvature

$$|F_{P\gamma\gamma}(0)|^2 = \frac{64\pi}{(4\pi\alpha)^2}\frac{\Gamma(P\to\gamma\gamma)}{m_P^3}$$

exp. decay width

or

$$F_{\pi^0\gamma\gamma}(0) = 1/(4\pi^2 F_\pi)$$

axial anomaly

(not for η and η')

@ large-momentum transfer:

$$F(Q^2) = \int T_H(x, Q^2)\Phi_P(x, \mu_F)\mathrm{d}x$$

$T_H(\gamma^*\gamma \to q\bar{q})$ $\quad$ $\Phi_P(q\bar{q} \to P)$

convolution of perturbative and non-perturbative regimes

@ lowest order in pQCD

$$Q^2F(Q^2) = \frac{\sqrt{2}f_\pi}{3}\int_0^1 \frac{dx}{x}\phi_\pi(x, Q^2) + O(\alpha_s) + O\left(\frac{\Lambda^2_{QCD}}{Q^2}\right),$$

$$Q^2F(Q^2) = \sqrt{2}f_\pi$$

- *Padé approximants*

$$Q^2 F_{\eta^{(\prime)}\gamma*\gamma}(Q^2,0) = a_0 Q^2 + a_1 Q^4 + a_2 Q^6 + \ldots$$

$$P_M^N(Q^2) = \frac{T_N(Q^2)}{R_M(Q^2)} = a_0 Q^2 + a_1 Q^4 + a_2 + Q^6 + \cdots + \mathcal{O}((Q^2)^{N+M+1})$$

$\Rightarrow$ simple, systematic and model-independent parametrization of experimental data in the whole energy range (better convergence)

Fitting method: use of different sequences of PAs

- *How many sequences?*

  depends on the analytic structure of the exact function

- *How many elements per sequence?*

  limited by exp. data points and statistical errors

• *Padé approximants*

P. Masjuan, S. Peris and J.J. Sanz-Cillero, PRD 78 (2008) 074028

P. Masjuan, PRD 86 (2012) 094021

How to ascribe a systematic error to the results?

test the method with a model → try different models

• *Log model:* $$F_{\pi^0\gamma^*\gamma}(Q^2) = \frac{M^2}{4\pi^2 f_\pi Q^2}\log\left(1+\frac{Q^2}{M^2}\right),$$

TABLE I. a_0, a_1, and a_2 low-energy coefficients of the log model in Eq. (3), fitted with a $P_1^L(Q^2)$ and its exact values (last column). We also include the prediction for the pole of each $P_1^L(Q^2)$ (s_p) to be compared with the lowest-lying meson in the model.

		P_1^0	P_1^1	P_1^2	P_1^3	P_1^4	P_1^5	$F_{\pi^0\gamma^*\gamma}$ (exact)	
	a_0 (GeV^{-1})	0.2556	0.2694	0.2734	0.2746	0.2751	0.2752	0.2753	
slope	a_1 (GeV^{-3})	0.1290	0.1716	0.1935	0.2051	0.2124	0.2166	0.2294	5.6% of sys. error
curvature	a_2 (GeV^{-5})	0.0651	0.1147	0.1492	0.1725	0.1898	0.2013	0.2549	21% of sys. error
	$\sqrt{s_p}$ (GeV)	1.41	1.22	1.14	1.09	1.05	1.03	0.77	

• *Regge model:* $$F_{\pi^0\gamma^*\gamma^*}(q_1^2, q_2^2) = \sum_{V_\rho, V_\omega} \frac{F_{V_\rho}(q_1^2)F_{V_\omega}(q_2^2)G_{\pi V_\rho V_\omega}(q_1^2, q_2^2)}{(q_1^2 - M_{V_\rho}^2)(q_2^2 - M_{V_\omega}^2)} + (q_1 \leftrightarrow q_2),$$

slope	a_1 (GeV^{-3})	0.2662	0.3121	0.3338	0.3457	0.3529	0.3571	0.3678	2.9% of sys. error
curvature	a_2 (GeV^{-5})	0.2652	0.3600	0.4244	0.4616	0.4868	0.5030	0.5550	9.4% of sys. error

- *Application to η and η' TFFs*

asymptotic behaviour

To use the P[N,1](Q^2) and P[N,N](Q^2) sequences of PAs

single resonance dominance

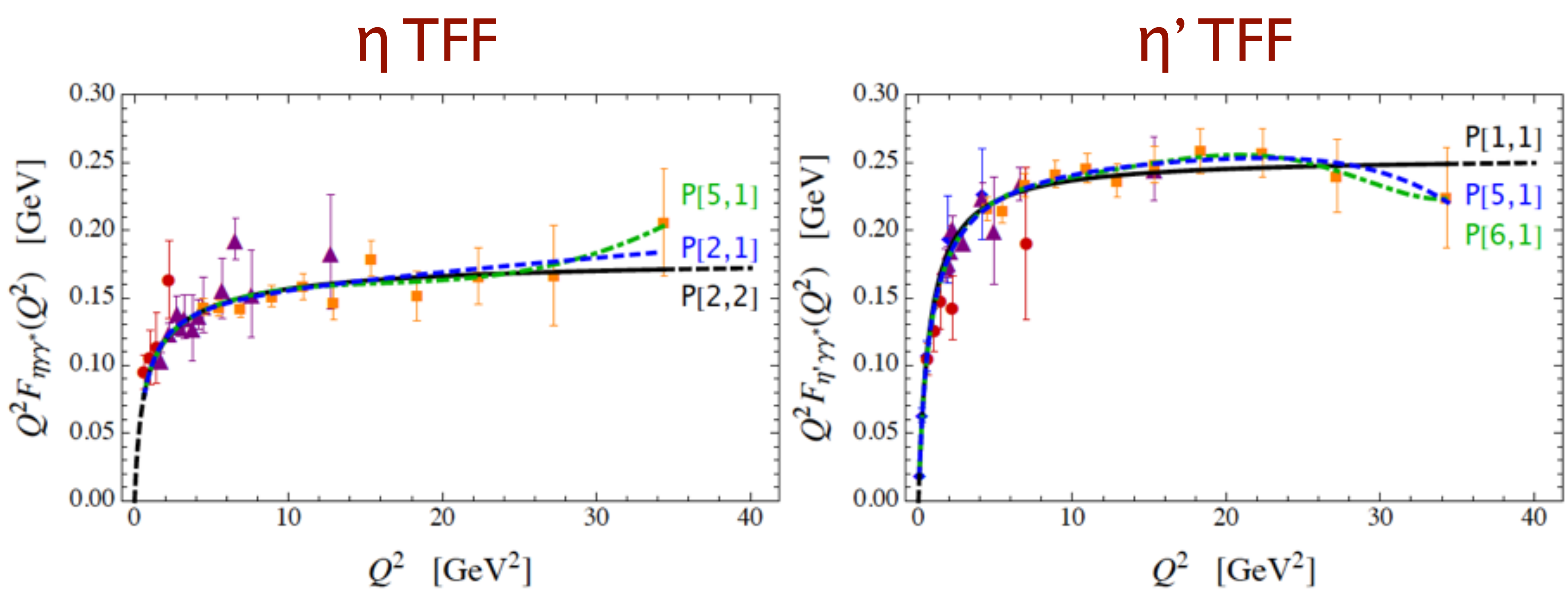

FIG. 1. η- and η'-TFFs best fits (left and right panels reps.). Blue dashed line shows our best $P_1^L(Q^2)$ when the two-photon partial decay width is *not* included in our set of data to be fitted. When the two-photon partial decay width *is* included, dark-green dot-dashed line shows our best $P_1^L(Q^2)$, and black solid line shows our best $P_N^N(Q^2)$. Black dashed lines are the extrapolation of such approximant at $Q^2 = 0$ and at $Q^2 \to \infty$. Data points are from CELLO (red circles) [28], CLEO (purple triangles) [36], L3 (blue diamonds) [31], and *BABAR* (orange squares) [30] Collaborations. See main text for details.

• *Application to η and η' TFFs*

Slope:

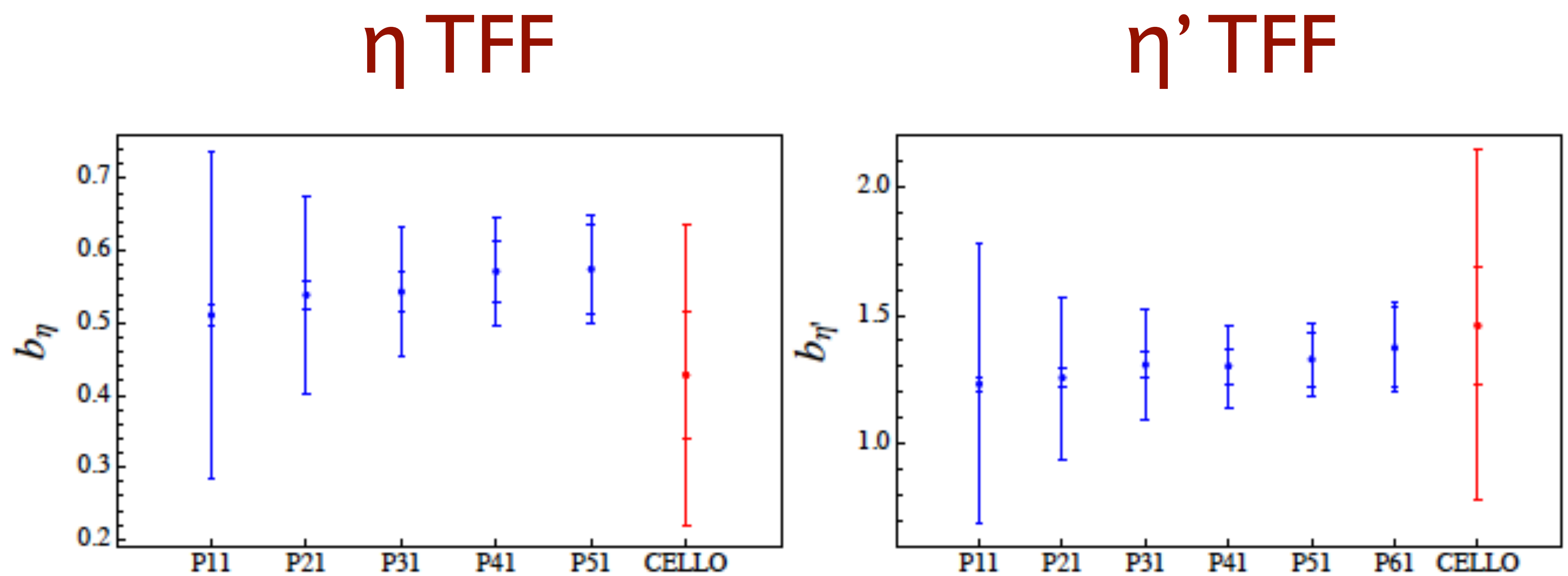

FIG. 2. Slope predictions with the $P_1^L(Q^2)$ up to $L = 5$ and $L = 6$ for the η-TFF and the η'-TFF (left and right panels respectively). The internal band is the statistical error from the fit and the external one is the combination of statistical and systematic errors determined in the previous section.

Curvature:

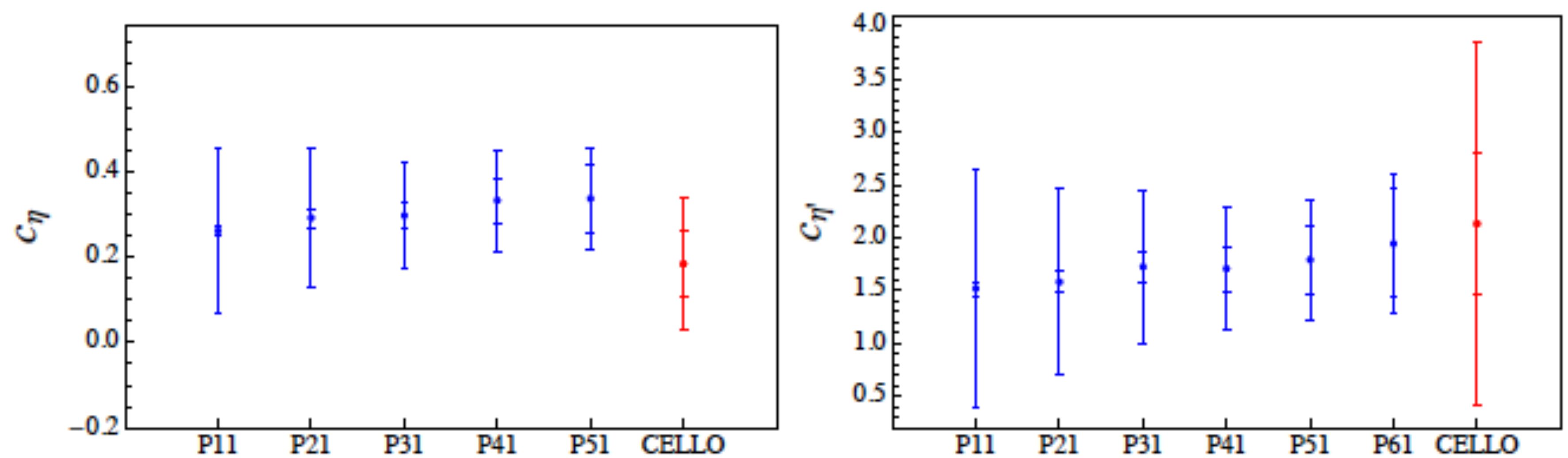

FIG. 3. Curvature predictions with the $P_1^L(Q^2)$ up to $L = 5$ and $L = 6$ for the η-TFF and the η'-TFF (left and right panels respectively). The internal band is the statistical error from the fit and the external one is the combination of statistical and systematic errors determined in the previous section.

- *Results*

Slope and curvature:

$$b_\eta = 0.596(48)_{stat}(33)_{sys}$$
$$c_\eta = 0.362(66)_{stat}(76)_{sys} \times 10^{-3}$$

$$b_{\eta'} = 1.37(16)_{stat}(8)_{sys}$$
$$c_{\eta'} = 1.94(52)_{stat}(41)_{sys} \times 10^{-3}$$

Comparison with other results:

$$F_{P\gamma^*\gamma}(Q^2) = \frac{F_{P\gamma\gamma}(0)}{1+Q^2/\Lambda_P^2}$$

ChPT: b_η=0.51, $b_{\eta'}$=1.47

CELLO: b_η=0.428(89), $b_{\eta'}$=1.46(23)

VMD: b_η=0.53, $b_{\eta'}$=1.33

CLEO: b_η=0.501(38), $b_{\eta'}$=1.24(8)

cQL: b_η=0.51, $b_{\eta'}$=1.30

Lepton-G: b_η=0.57(12), $b_{\eta'}$=1.6(4)

BL: b_η=0.36, $b_{\eta'}$=2.11

NA60: b_η=0.585(51)

$$\mathcal{F}_{\gamma^*\gamma\mathcal{R}}(Q^2) \sim \frac{1}{4\pi^2 f_\mathcal{R}} \frac{1}{1+(Q^2/8\pi^2 f_\mathcal{R}^2)}$$

MAMI: b_η=0.58(11), WASA: b_η=0.68(26)

Disp: b_η=0.61(+0.07)(-0.03), $b_{\eta'}$=1.45(+0.17)(-0.12)

$\eta,\eta' \to \gamma^*\gamma$

- *Further applications of this method*

Analysis of time-like processes ($\eta,\eta' \to l^+l^-\gamma$)

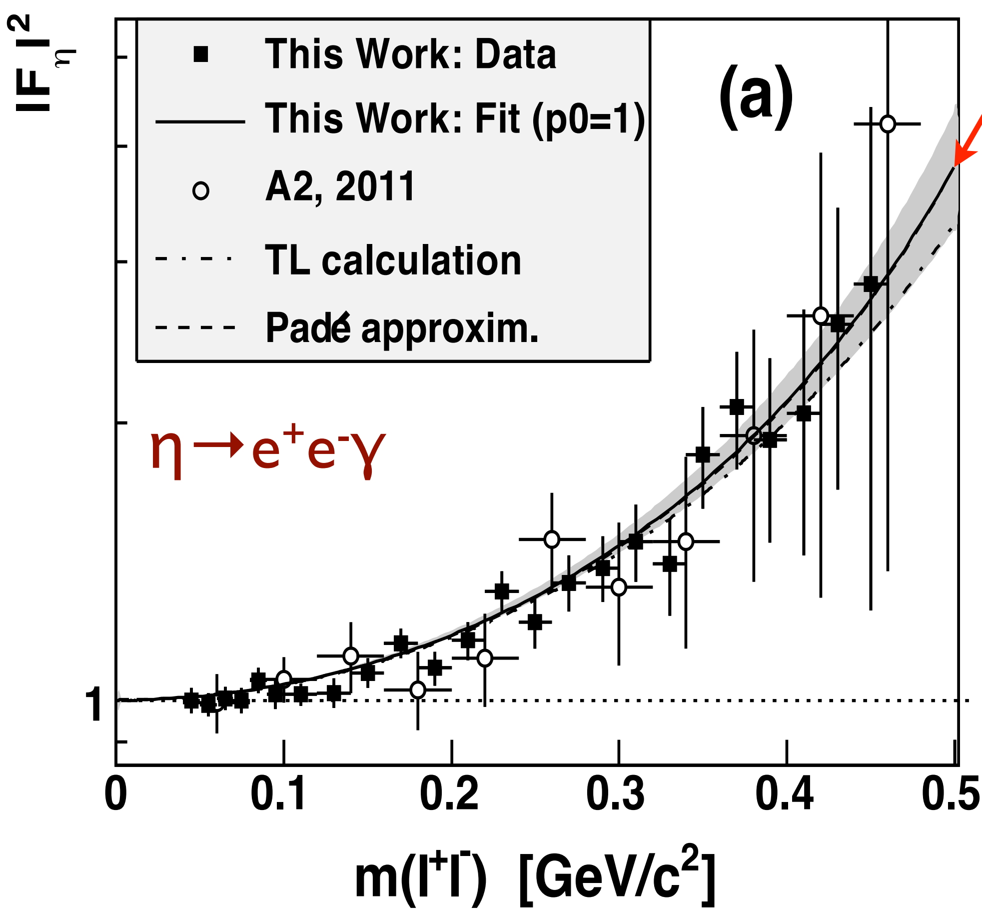

Our *prediction* is *behind* the experimental fit!

PREVIOUS RESULTS
$b_\eta = 0.596(48)(33)$,
$c_\eta = 0.362(66)(76)$
Asymptotics $= 0.164(21)$ GeV

Adding MAMI data to our fit

UPDATED RESULTS
(PRELIMINARY RESULTS)
$b_\eta = 0.588(27)(25)$,
$c_\eta = 0.357(38)(61)$
Asymptotics $= 0.174(15)$ GeV

M. Unverzagt et al. (A2 Coll. @MAMI), PRC 89 (2014) 044608

Analysis of π^0, η and η' contributions to HLbL of $(g-2)_\mu$

- *Application to η TFF in the time-like region*

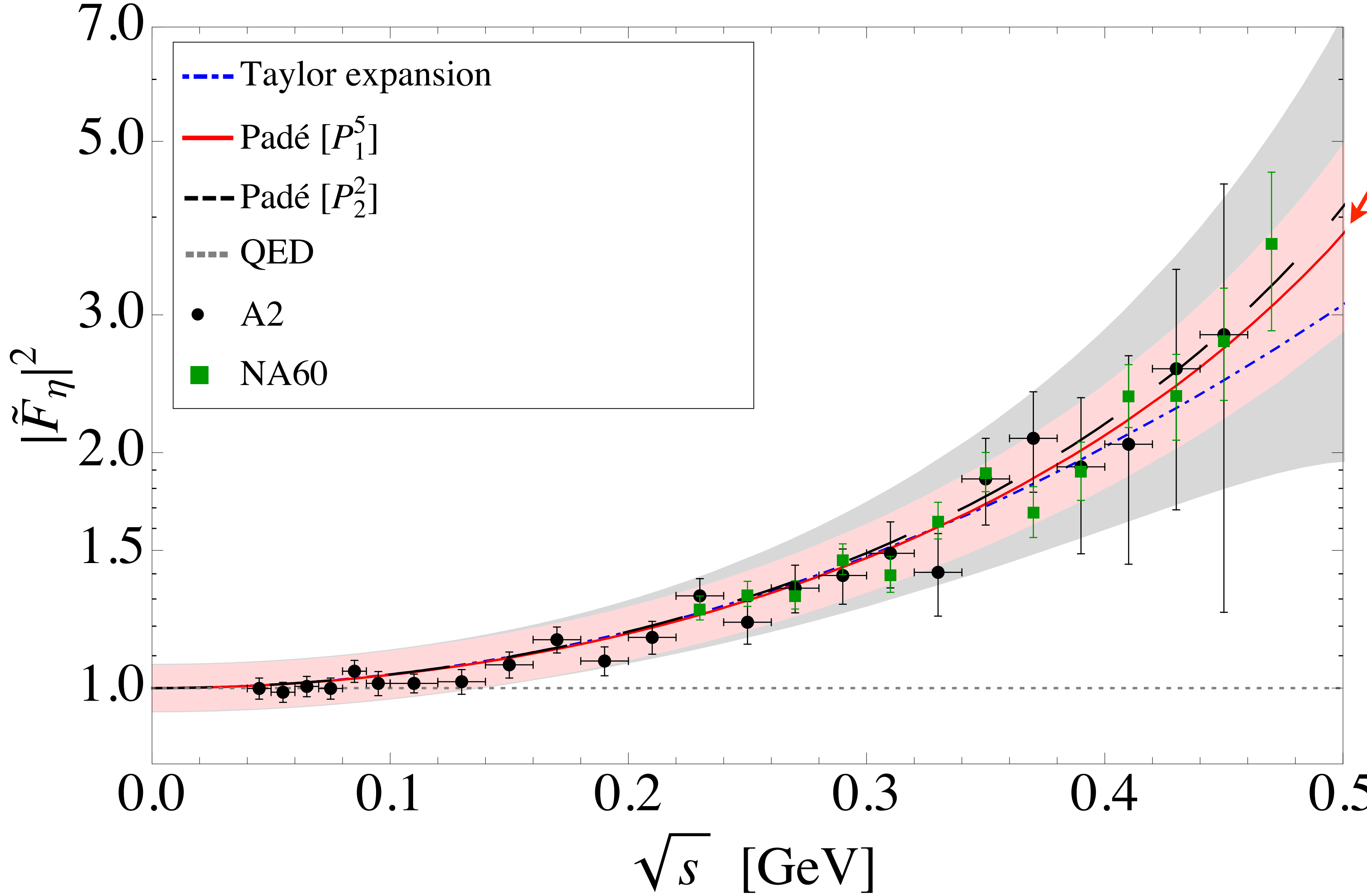

Our *predictions* not fits!

Figure 1. Modulus square of the normalized time-like η TFF, $\widetilde{F}_{\eta\gamma\gamma^*}(q^2)$, as a function of the invariant dilepton mass, $\sqrt{s} \equiv m_{\ell\ell}$. The predictions coming from the $P^5_1(q^2)$ (red solid line) and $P^2_2(q^2)$ (black long-dashed line) PAs, and the Taylor expansion (blue dot-dashed line) are compared to the experimental data from $\eta \to e^+e^-\gamma$ [4] (black circles) and $\eta \to \mu^+\mu^-\gamma$ [7] (green squares). The one-sigma error bands associated to $P^5_1(q^2)$ (light-red) and $P^2_2(q^2)$ (light-gray) PAs, and the QED prediction (gray short-dashed line) are also displayed.

• *Application to η' TFF in the time-like region*

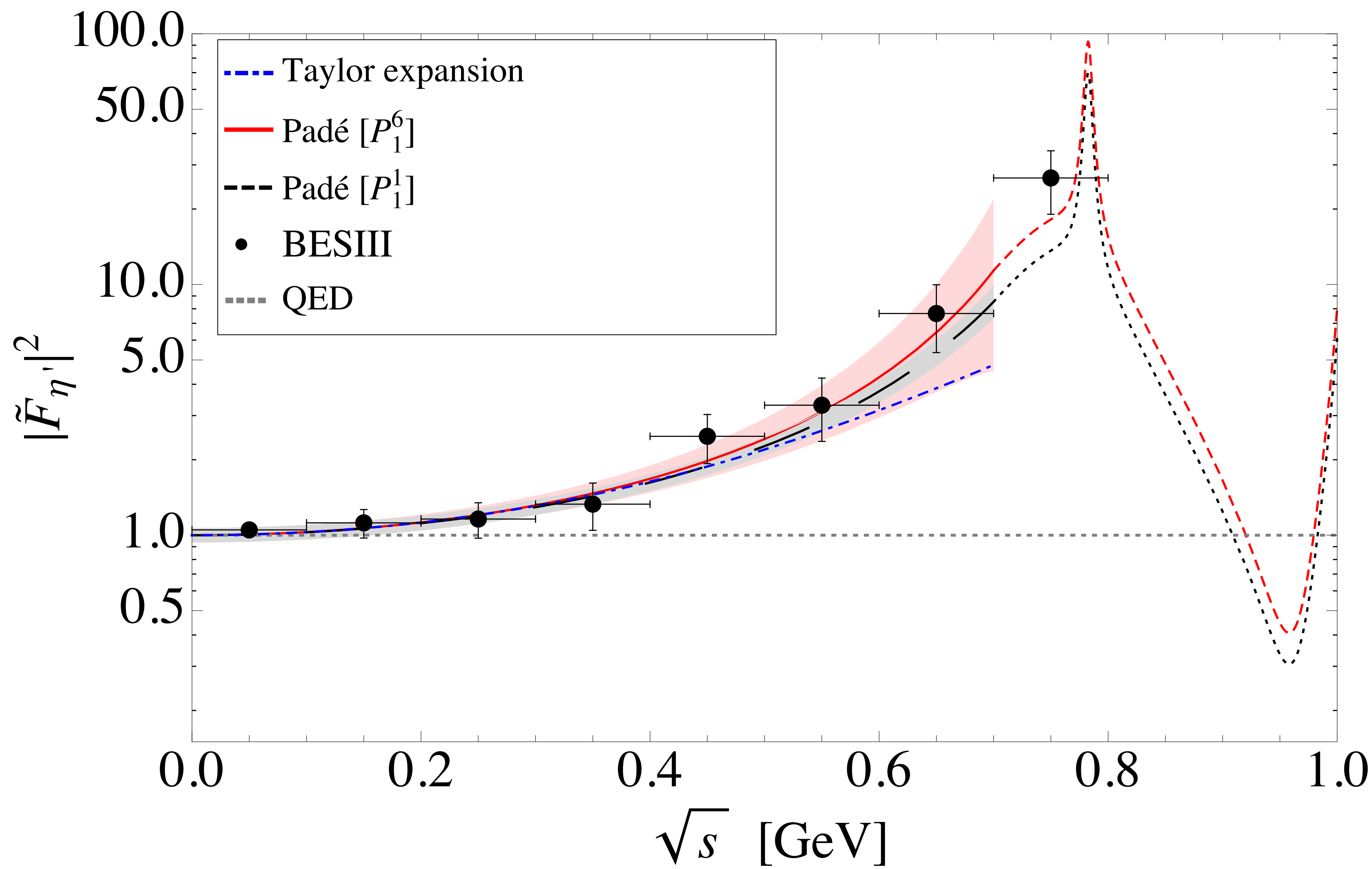

Figure 2. Modulus square of the normalized time-like η' TFF, $\widetilde{F}_{\eta'\gamma\gamma^*}(q^2)$, as a function of the invariant dilepton mass, $\sqrt{s} \equiv m_{\ell\ell}$. The predictions up to the matching point located at $\sqrt{s} = 0.70$ GeV coming from the $P_1^6(q^2)$ (red solid line) and $P_1^1(q^2)$ (black long-dashed line) PAs, and the Taylor expansion (blue dot-dashed line) are compared to the experimental data from $\eta' \to e^+e^-\gamma$ [8] (black circles). From the matching point on, rescaled versions of the VMD description in eq. (1.4) are used. The one-sigma error bands associated to $P_1^6(q^2)$ (light-red) and $P_1^1(q^2)$ (light-gray) PAs, and the QED prediction (gray short-dashed line) are also displayed.

- *Application to η' TFF in the time-like region*

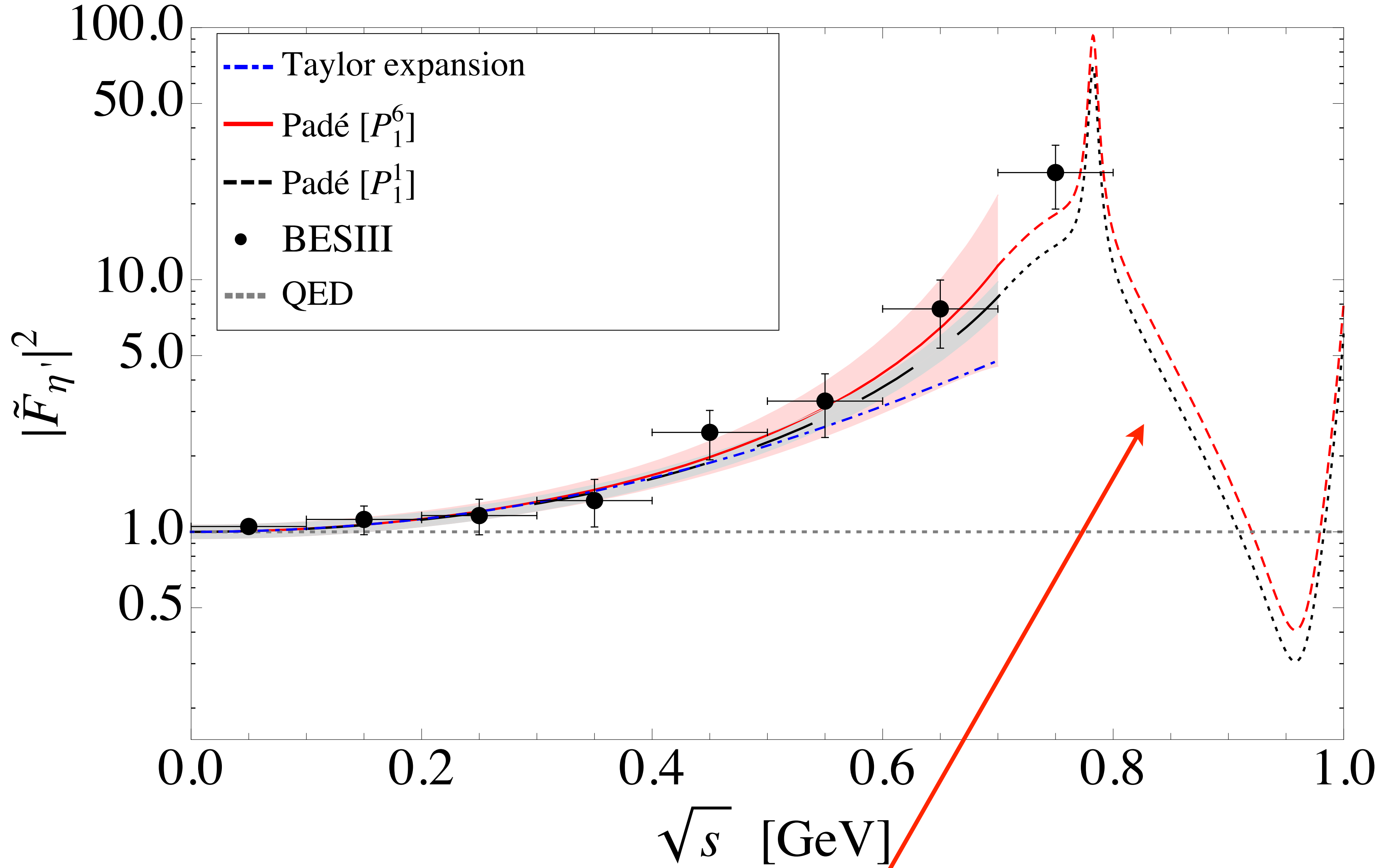

L. G. Landsberg, Phys. Rept. 128 (1985) 301

$$\widetilde{F}_{\mathcal{P}\gamma\gamma^*}(q^2) = \left(\sum_{V=\rho,\omega,\phi} \frac{g_{V\mathcal{P}\gamma}}{2g_{V\gamma}} \right)^{-1} \sum_{V=\rho,\omega,\phi} \frac{g_{V\mathcal{P}\gamma}}{2g_{V\gamma}} \frac{M_V^2}{M_V^2 - q^2 - iM_V\Gamma_V(q^2)}$$

- *Single Dalitz decays*

$\eta \to l^+ l^- \gamma$ ($l = e, \mu$)

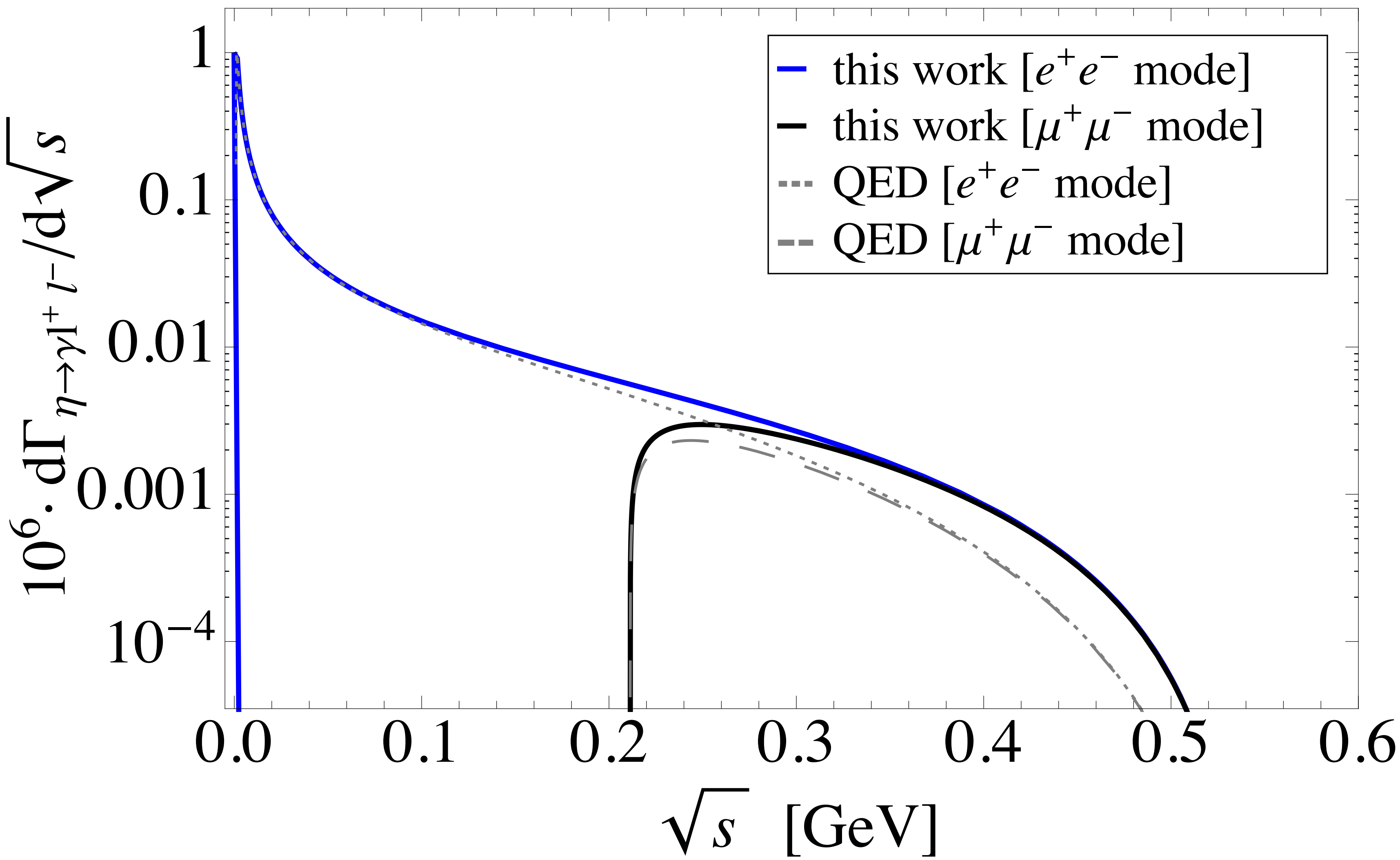

Figure 3. Decay rate distribution for $\eta \to e^+e^-\gamma$ (blue solid curve) and $\eta \to \mu^+\mu^-\gamma$ (black solid curve). The corresponding QED estimates are also displayed (gray dotted and long-dashed curves, respectively).

- *Single Dalitz decays*

$\eta \to l^+ l^- \gamma$ ($l = e, \mu$)

Source	$\mathcal{BR}(\eta \to e^+e^-\gamma)\cdot 10^3$	$\mathcal{BR}(\eta \to \mu^+\mu^-\gamma)\cdot 10^4$
this work $[P_1^5]$	$6.60^{+0.50}_{-0.46}$	$3.25^{+0.37}_{-0.33}$
this work $[P_2^2]$	$6.61^{+0.53}_{-0.49}$	$3.30^{+0.62}_{-0.54}$
QED	6.38	2.17
Experimental measurements	6.9(4)[1] $6.6(4)_{\rm stat}(4)_{\rm syst}$ [3] $6.72(7)_{\rm stat}(31)_{\rm syst}$ [6]	3.1(4) [1]

Table 1. Comparison between our $\mathcal{BR}$ predictions for $\eta \to \ell^+\ell^-\gamma$ and experimental measurements.

[1] PDG, Chin. Phys. C38 (2014) 090001

[3] H. Berghauser, Phys. Lett. B701 (2011) 562

[6] P. Adlarson *et. al.*, arXiv:1509.06588 [nucl-ex]

- *Single Dalitz decays*

$\eta' \to l^+ l^- \gamma$ ($l = e, \mu$)

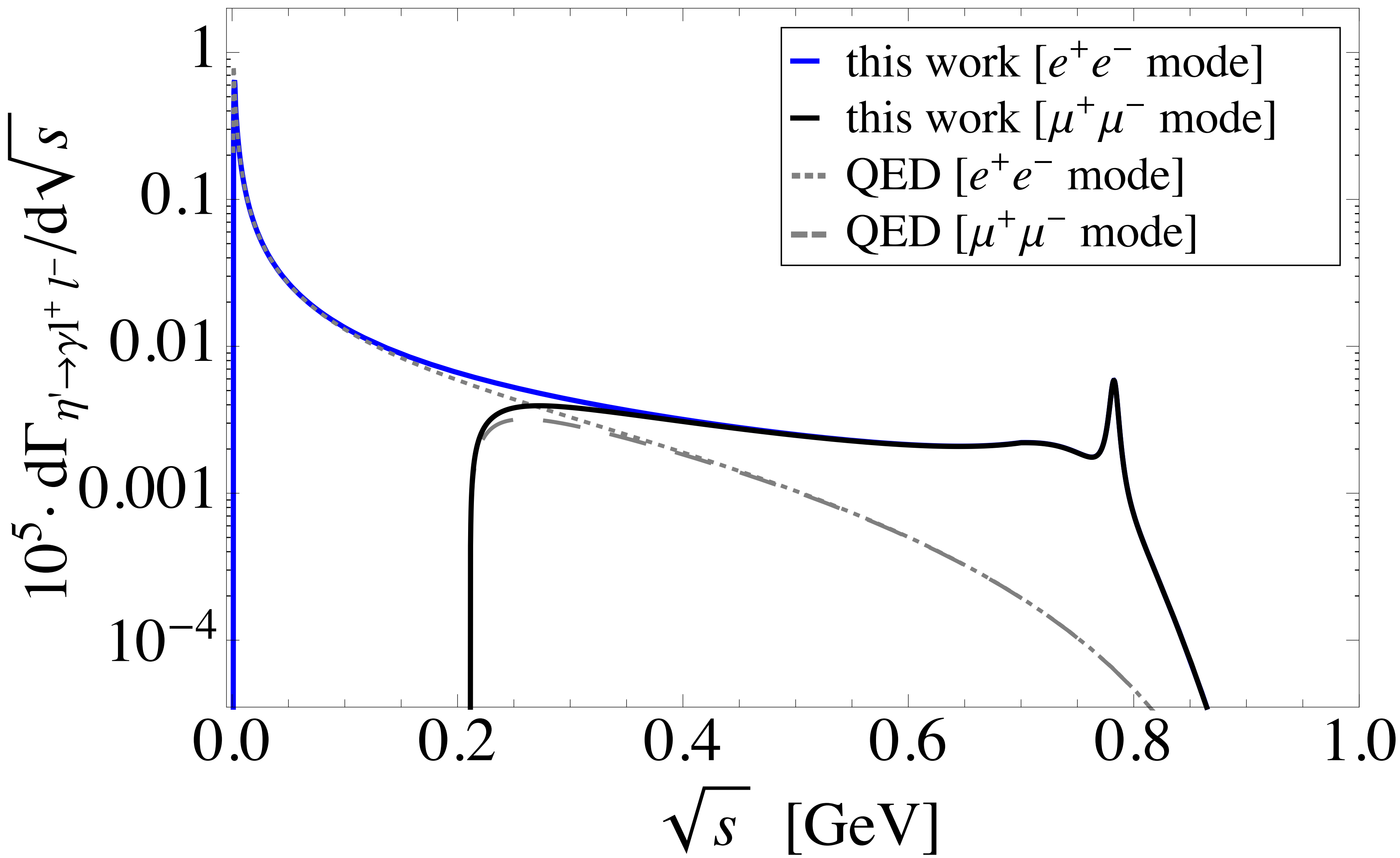

Figure 4. Decay distributions for $\eta' \to e^+e^-\gamma$ (blue solid curve) and $\eta' \to \mu^+\mu^-\gamma$ (black solid curve). The QED estimates are also shown (gray dotted and long-dashed curves, respectively).

- *Single Dalitz decays*

$\eta' \to l^+ l^- \gamma$ ($l = e, \mu$)

Source	$\mathcal{BR}(\eta' \to e^+e^-\gamma)\cdot 10^4$	$\mathcal{BR}(\eta' \to \mu^+\mu^-\gamma)\cdot 10^4$
this work $[P_1^6]$	$4.42^{+0.38}_{-0.34}$	$0.81^{+0.15}_{-0.12}$
this work $[P_1^1]$	$4.35^{+0.28}_{-0.26}$	$0.74(5)$
QED	3.94	0.38
Experimental measurements	$4.69(20)_{\rm stat}(23)_{\rm sys}$ [8]	$1.08(27)$ [9]

Table 2. Comparison between our $\mathcal{BR}$ predictions for $\eta' \to \ell^+\ell^-\gamma$ and experimental measurements.

[8] M. Ablikim *et. al.* (BESIII Coll.), Phys. Rev. D 92 (2015) 1, 012001

[9] R. I. Dzhelyadin et al., Sov. J. Nucl. Phys. 32 (1980) 520

- *Double Dalitz decays*

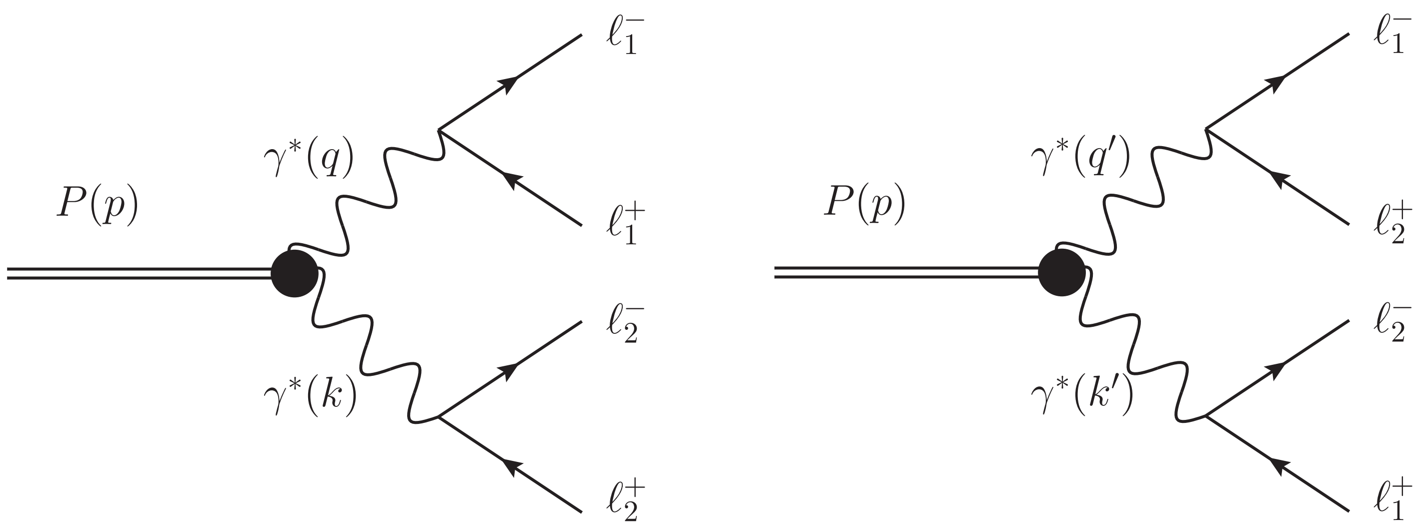

Figure 5. Double Dalitz direct (left) and exchange (right) diagrams.

Bivariate approximants:

Standard Factorisation approach

$$\widetilde{F}_{\mathcal{P}\gamma^*\gamma^*}(q_1^2, q_2^2) = \widetilde{F}_{\mathcal{P}\gamma\gamma^*}(q_1^2, 0)\widetilde{F}_{\mathcal{P}\gamma\gamma^*}(0, q_2^2)$$

Chisholm approximants

$$P_1^0(q_1^2, q_2^2) = \frac{a_{0,0}}{1 - \frac{b_{1,0}}{M_{\mathcal{P}}^2}(q_1^2 + q_2^2) + \frac{b_{1,1}}{M_{\mathcal{P}}^4} q_1^2 q_2^2}$$

- *Double Dalitz decays*

$\eta \to e^+e^-\mu^+\mu^-$

[5] M. Berlowski et al. (CELSIUS/WASA Coll.), Phys. Rev. D 77 (2008) 032004

Source	Double-virtual TFF		$\mathcal{BR}(\eta \to e^+e^-\mu^+\mu^-) \cdot 10^6$
This work	Chisholm approximants	$b_{1,1} = 0$	2.39(12)
		$b_{1,1} = b_{1,0}$	2.39(12)
		$b_{1,1} = 2b_{1,0}$	2.38(12)
	factorisation approach	P_1^5	$2.35^{+0.45}_{-0.38}$
		P_2^2	$2.39^{+0.64}_{-0.51}$
	QED		1.57
Experimental measurement			$< 1.6 \cdot 10^{-4}$ (90% CL) [5]

$\eta \to l^+l^-l^+l^-$ ($l=e,\mu$)

[6] P. Adlarson *et. al.*, arXiv:1509.06588 [nucl-ex]
[11] F. Ambrosino et al. (KLOE & KLOE-2 Colls.), Phys. Lett. B 702 (2014) 324

Source	TFF		$\mathcal{BR}(\eta \to e^+e^-e^+e^-) \cdot 10^5$		$\mathcal{BR}(\eta \to \mu^+\mu^-\mu^+\mu^-) \cdot 10^9$	
			dir+exch	inter	dir+exch	inter
This work	CAs	$b_{1,1} = 0$	2.74(3)	-0.02	4.47(26)	-0.32
		$b_{1,1} = b_{1,0}$	2.73(3)	-0.03	4.31(26)	-0.32
		$b_{1,1} = 2b_{1,0}$	2.73(3)	-0.03	4.15(26)	-0.32
	fact.	P_1^5	$2.72^{+0.42}_{-0.37}$	-0.03	$4.23^{+0.79}_{-0.67}$	-0.43
		P_2^2	$2.73^{+0.45}_{-0.38}$	-0.03	$4.30^{+1.08}_{-0.88}$	-0.47
	QED		2.56	-0.02	2.59	-0.19
Exp. measurements			$3.2(9)_{\rm stat}(5)_{\rm sys}$ [6] $2.4(2)_{\rm stat}(1)_{\rm sys}$ [11]		$< 3.6 \cdot 10^{-4}$ (90% CL) [5]	

- *Double Dalitz decays*

$\eta' \to e^+e^-\mu^+\mu^-$

Source	$\mathcal{BR}(\eta' \to \mu^+\mu^-e^+e^-) \cdot 10^7$
this work $[P_1^6]$	$6.80^{+1.31}_{-1.12}$
this work $[P_1^1]$	$6.25^{+0.76}_{-0.66}$
QED	3.21
Experimental measurements	not seen

$\eta' \to l^+l^-l^+l^-$ $(l=e,\mu)$

Source	TFF		$\mathcal{BR}(\eta' \to e^+e^-e^+e^-) \cdot 10^6$		$\mathcal{BR}(\eta' \to \mu^+\mu^-\mu^+\mu^-) \cdot 10^8$	
			direct+exch	inter	direct+exch	inter
This work	factorisation	P_1^6	$2.15^{+0.34}_{-0.29}$	-0.03	$2.19^{+0.22}_{-0.18}$	-0.44
		P_1^1	$2.09^{+0.27}_{-0.24}$	-0.01	$2.06^{+0.15}_{-0.14}$	-0.41
	QED		1.75	-0.01	0.98	-0.11
Exp. measurements			not seen		not seen	

- *Summary and Conclusions*

We have analyzed the π^0, η and η' single and double Dalitz decays by means of a data-driven model-independent approach based on the use of rational approximants

The π^0, η and η' transition form factors were obtained from experimental data at low and intermediate energies in the space-like region

We have obtained accurate values of the corresponding dilepton invariant mass spectra and branching ratios

More experimental data would be desirable (BESIII, BELLE?, KLOE, WASA) to further improve this method

• *Summary and Conclusions*

Decay	This work	Experimental value [1]	n_σ
$\pi^0 \to e^+e^-\gamma$	$1.169(1)\%$	$1.174(35)\%$	0.15
$\eta \to e^+e^-\gamma$	$6.61(59)\cdot 10^{-3}$	$6.90(40)\cdot 10^{-3}$	0.41
$\eta \to \mu^+\mu^-\gamma$	$3.27(56)\cdot 10^{-4}$	$3.1(4)\cdot 10^{-4}$	0.25
$\eta' \to e^+e^-\gamma$	$4.38(31)\cdot 10^{-4}$	$4.69(20)(23)\cdot 10^{-4}$	0.49
$\eta' \to \mu^+\mu^-\gamma$	$0.74(5)\cdot 10^{-4}$	$1.08(27)\cdot 10^{-4}$	1.24
$\pi^0 \to e^+e^-e^+e^-$	$3.36689(5)\cdot 10^{-5}$	$3.34(16)\cdot 10^{-5}$	0.17
$\eta \to e^+e^-e^+e^-$	$2.71(2)\cdot 10^{-5}$	$2.4(2)(1)\cdot 10^{-5}$	0.66
$\eta \to \mu^+\mu^-\mu^+\mu^-$	$3.98(15)\cdot 10^{-9}$	$< 3.6\cdot 10^{-4}$	
$\eta \to e^+e^-\mu^+\mu^-$	$2.39(7)\cdot 10^{-6}$	$< 1.6\cdot 10^{-4}$	
$\eta' \to e^+e^-e^+e^-$	$2.14(45)\cdot 10^{-6}$	not seen	
$\eta' \to \mu^+\mu^-\mu^+\mu^-$	$1.69(35)\cdot 10^{-8}$	not seen	
$\eta' \to e^+e^-\mu^+\mu^-$	$6.39(87)\cdot 10^{-7}$	not seen	

Table 8. Central final branching ratio predictions as a combined weighted average of the results presented. Errors are symmetrised. n_σ stands for the number of standard deviations the measured results are from our predictions.